NANO LETTERS

LETTER

pubs.acs.org/NanoLett

High, Size-Dependent Quality Factor in an Array of Graphene Mechanical Resonators

Robert A. Barton,[†] B. Ilic,[‡] Arend M. van der Zande,[§] William S. Whitney,[§] Paul L. McEuen,[§,∥] Jeevak M. Parpia,[§] and Harold G. Craighead[*,†]

[†]School of Applied and Engineering Physics, [‡]Cornell NanoScale Science and Technology Facility, [§]Laboratory of Atomic, Solid State Physics, and [∥]Kavli Institute at Cornell for Nanoscale Science, Cornell University, Ithaca, New York 14853, United States

Supporting Information

ABSTRACT: Graphene's unparalleled strength, stiffness, and low mass per unit area make it an ideal material for nanomechanical resonators, but its relatively low quality factor is an important drawback that has been difficult to overcome. Here, we use a simple procedure to fabricate circular mechanical resonators of various diameters from graphene grown by chemical vapor deposition. In addition to highly reproducible resonance frequencies and mode shapes, we observe a striking improvement of the membrane quality factor with increasing size. At room temperature, we observe quality factors as high as 2400 ± 300 for a resonator 22.5 μm in diameter, about an order of magnitude greater than previously observed quality factors for monolayer graphene. Measurements of quality factor as a function of modal frequency reveal little dependence of Q on frequency. These measurements shed light on the mechanisms behind dissipation in monolayer graphene resonators and demonstrate that the quality factor of graphene resonators relative to their thickness is among the highest of any mechanical resonator demonstrated to date.

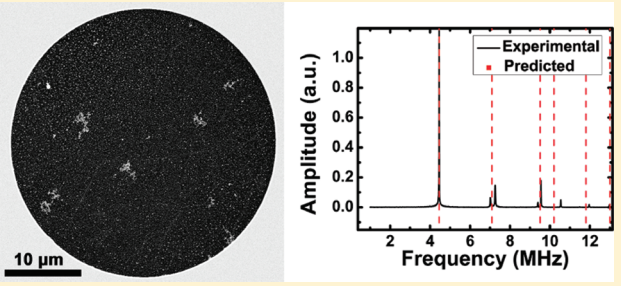

KEYWORDS: Graphene, nanoelectromechanical systems (NEMS), quality factor, dissipation

The impressive precision of nanomechanical resonators as sensors of mass,[1] force,[2] and position[3] relies on their having both small cross-sectional dimensions and a high quality factor. For example, the minimum mass detectable with a resonant sensor against a background of white noise is[4]

$$\Delta m_{\mathrm{min}} = 2\left(\frac{m_{\mathrm{eff}}}{Q}\right)10^{-\mathrm{DR}/20} \qquad (1)$$

where m_{eff} is the effective mass of the resonator, Q is the mechanical quality factor of the resonator, and DR is the dynamic range in dB. Unfortunately, while it is possible to improve the sensitivity of resonators by reducing their cross-sectional dimensions, the gains are generally offset by decreases in Q because for small dimensions, Q decreases from surface effects.[5] More quantitatively, studies of NEMS show that Q is inversely proportional to surface area to volume ratio R, so the magnitude of a resonator's RQ product is a good indicator of its performance at small sizes.[6] For conventional nanomechanical materials such as single crystal silicon, RQ products are on the order of 1000 nm^{-1} or less. Interestingly, it appears that the problems associated with surface effects can be overcome by new materials; for example, stoichiometric silicon nitride under high tensile strain[7] has demonstrated $RQ \sim 30\,000$ nm^{-1} as a doubly clamped beam[8] and $RQ \sim 100\,000$ nm^{-1} as a membrane.[9] However, silicon nitride also has drawbacks as a nanomechanical material; most importantly, it is not electrically conductive and therefore requires modification to enable electrical readout.[10] The ideal nanomechanical material would have high Q, low mass, and good signal-to-noise with integrated readout.

Low-dimensional carbon allotropes offer a unique alternative to traditional CMOS materials as building blocks for resonators with small cross sectional dimensions,[11,12] In particular, resonators made of graphene, which were first manufactured in 2007,[13] show much promise. In addition to having extraordinarily low mass, graphene is strong, stiff,[14] and electrically conductive, which provides a route to high signal-to-noise with electrical integration.[15] Furthermore, graphene's planar geometry is amenable to standard fabrication techniques. However, the quality factor of graphene resonators has been among the lowest of nanoelectromechanical systems made to date. Until now, the highest quality factor observed in monolayer graphene resonators at room temperature[13,15−18] was on the order of several hundred. Even relative to graphene's small thickness, this Q is unimpressive. Assuming a thickness of 0.335 nm,[19] graphene resonators demonstrated to date have RQ products less than 2000 nm^{-1}. Thicker variants of graphene, like graphene oxide[20] ($Q \sim 4000$) and multilayer epitaxially grown graphene[21] ($Q \sim 1000$) have

Received: December 3, 2010
Revised: January 10, 2011

   dx.doi.org/10.1021/nl1042227 | *Nano Lett.* XXXX, XXX, 000–000

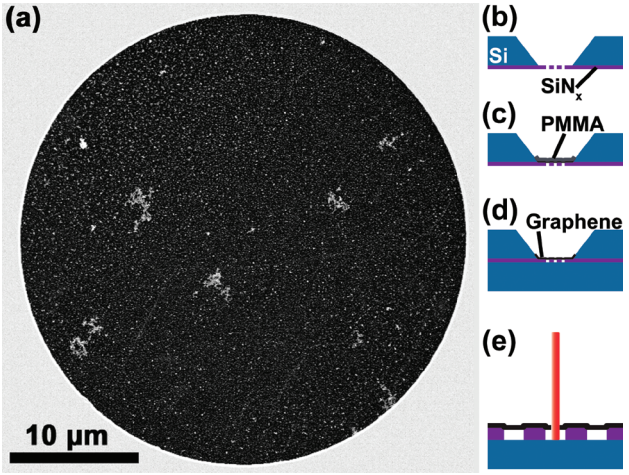

Figure 1. (a) SEM image of a suspended circular graphene membrane 30 μm in diameter. (b−d) Schematic of the fabrication procedure used to make the membrane in (a). Graphene on PMMA is transferred to a nitride membrane, the PMMA is decomposed, and the nitride is pressed flush against a polished silicon wafer. (e) Diagram of the interferometric apparatus used to detect resonator motion.

demonstrated higher quality factors but not higher RQ products. Despite the many advantages of graphene as a nanomechanical material, dissipation in graphene resonators is poorly understood and there has been little progress in overcoming it.

Here, we demonstrate that the low quality factors observed in graphene resonators can be substantially improved using modern fabrication techniques. We find that for circular graphene drum resonators fabricated by recently published chemical vapor deposition (CVD) methods, the quality factor is linearly dependent on the diameter of the resonator. We use this effect to produce resonators with Q as high as 2400 ± 300 at room temperature. These resonators have RQ products as high as 14 000 nm^{-1}, which rivals that of the best membrane resonators available today. Measurements of quality factor for different resonant modes suggest that Q is only weakly dependent on modal frequency and is determined predominantly by the size of the membrane. Together, these observations offer new insights into the dissipation mechanisms underlying graphene resonator performance.

Membranes such as the one shown in Figure 1a were fabricated following the procedure described in ref 17. Graphene was grown on copper foil by CVD.[22] After a 30−50 nm thick layer of poly(methyl methacrylate) (PMMA) was spin-coated on the graphene to mediate transfer, the copper was dissolved in a ferric chloride-based etch (CE-200, Transene) and the graphene was rinsed in DI H_2O. Separately, a Si substrate coated with ∼300 nm thick Si-rich silicon nitride was back-etched using KOH to suspend a 2 mm × 2 mm square nitride membrane. Then, using photolithography, circular holes were patterned in the nitride membrane with diameter 2−30 μm (Figure 1b). Following ref 22, the graphene was transferred to the backside of this substrate from the H_2O bath (Figure 1c). The graphene conformed to the substrate and adhered directly to the nitride membrane, covering many of the holes. After the graphene was allowed to dry in air, the PMMA was removed by decomposition at 350 °C in air.[23] This procedure resulted in suspended graphene drums with yields greater than 90% for holes 2 μm in diameter and as high as 25% for holes 30 μm in diameter. An example is shown in Figure 1a. We point out that localized contamination is visible on the surface of the graphene sheet. Transmission electron microscopy studies of graphene membranes prepared in an identical manner in ref 24 found that the bulk of the visible contamination was iron, oxygen, and carbon. However, the structural element of these resonators is monolayer graphene, as is evident from Raman spectroscopy (Supporting Information).

Finally, we allowed the front side of the nitride wafer to adhere to a blank piece of silicon. This step left graphene membranes up to 30 μm in diameter suspended on silicon nitride 300 nm above a silicon surface (see Figure 1d,e). Fixing the nitride membrane against the substrate was the crucial step that enabled us to measure quality factor in this work but not in the similar membranes of ref 17. Surprisingly, we found no membranes that stuck to the silicon backplane as a result of this step.

To detect the resonance of the graphene drums, we used an interferometric method described previously.[13,25,26] Resonator motion is monitored by a HeNe laser reflecting from the resonator and the silicon backplane; the interference between these two reflections changes when the resonator moves and thereby changes the total reflected light intensity. These changes are monitored by a fast photodiode connected to a spectrum analyzer. Resonator motion is actuated using a 405 nm amplitude-modulated diode laser (Picoquant, Berlin, Germany) that excites motion through photothermal expansion and contraction of the graphene membrane. All resonance measurements were performed in a vacuum chamber evacuated to pressures less than 6×10^{-3} Torr, where viscous damping was found to be insignificant.

We investigated both the spectra and fundamental modes of membranes of various sizes. As reported previously,[17] we found that clamping the membranes on all sides made the distribution of higher resonance modes relative to the fundamental modes predictable. A spectrum from one membrane that falls particularly close to a predicted spectrum is shown in Figure 2a. The dotted red lines show the predicted frequencies of all modes given the fundamental mode of the membrane (modes are expected at 1.59, 2.14, 2.30, 2.65, and 2.92 times the fundamental frequency).[27] Multiple peaks often cluster around the predicted frequency of a given mode, as for the second and third modes in Figure 2a. We attribute these peaks to theoretically degenerate modes whose degeneracy has been lifted by asymmetries in either the surface contamination or stress profile of the membranes. Figure 2b shows a histogram of the number of modes at a given multiple of the fundamental frequency for a set of 29 devices of various sizes; again, the peaks agree fairly well with theory. Measurements of the mode shapes of these circular membranes, obtained by measuring response amplitude as a function of laser position, confirm that the shapes of at least the first few modes are as predicted by the theory for circular membranes. Mode shape data for one membrane is presented in Figure 2c. This behavior should be contrasted with previous measurements of doubly clamped beam resonators made from exfoliated graphene, which frequently displayed complicated, unpredictable mode shapes.[28]

In addition to the well-behaved spectra of these devices, we found that the fundamental frequency as a function of device size was well described by a tensioned membrane model. In Figure 3a, we plot the fundamental frequency as a function of diameter for the set of 29 devices examined in Figure 2b. For circular

dx.doi.org/10.1021/nl1042227 |*Nano Lett.* XXXX, XXX, 000–000

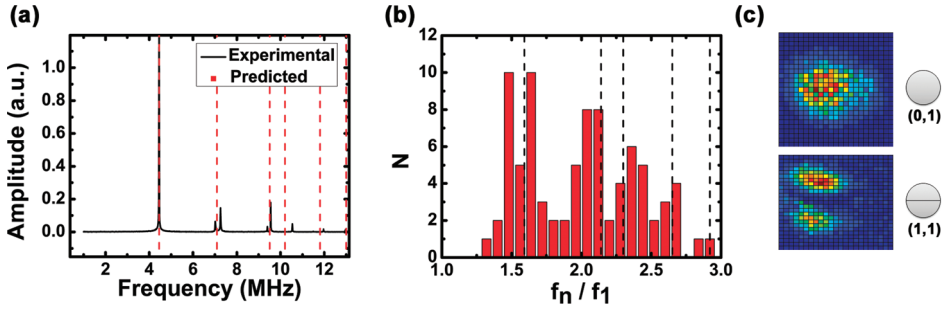

Figure 2. (a) Mechanical resonance spectrum for a circular graphene membrane (black) against the predicted location of all modes relative to the fundamental (red). (b) Histogram of the frequencies of all high order modes divided by the fundamental mode frequency for a set of 29 devices of various sizes. Black dotted lines show the expected frequency ratios for a circular membrane. (c) Amplitude of the resonance peak as a function of spatial position for the first two modes of a circular graphene membrane 22.5 μm in diameter. On gray circles, expected nodes for these modes are shown.

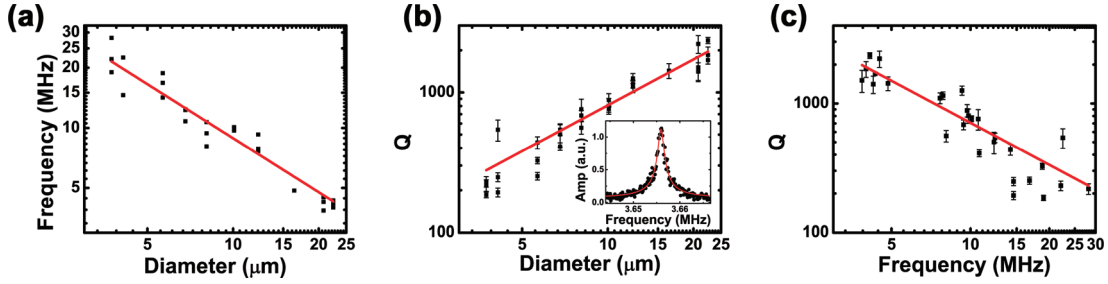

Figure 3. (a) Fundamental frequency f as a function of diameter D for the same set of devices studied in Figure 2b. The red line is a fit to the data revealing $f \sim D^{-0.9\pm0.1}$. (b) Quality factor of these graphene membranes as a function of diameter. The error bars represent the standard deviation in Q among six separate measurements of the width of the peak. The red line is a fit to the data revealing $Q \sim D^{1.1\pm0.1}$. Inset, the highest quality factor peak observed with a Lorentzian fit revealing $Q = 2400 \pm 300$. (c) Quality factor as a function of frequency for the same devices plotted in (a) and (b).

membranes under tension, the fundamental frequency should follow[27]

$$f = \frac{4.808}{2\pi D}\sqrt{\frac{Yt\varepsilon}{\rho\alpha}} \qquad (2)$$

where D is the diameter, Yt is the in-plane Young's modulus, ρ is the in-plane density of graphene, ε is the strain, and α is a density multiplier used to quantify the amount of mass contaminating the device ($\rho\alpha$ is defined to be the in-plane density of the resonator including both graphene and any additional mass). A fit of the data in Figure 3a shows that frequency is roughly proportional to inverse diameter as predicted by this equation. If we assume the known values for graphene, Yt = 340 N/m and $\rho = 7.4 \times 10^{-16}$ g μm^{-2}, we find that $\varepsilon/\alpha \sim 10^{-5}$. Since the density of the resonator is at least that of graphene ($\alpha > 1$), the minimum possible strain in the graphene is 10^{-5}, which is comparable to the strain in previously fabricated graphene resonators.[13] The tension is thought to be caused by the adherence of the graphene to the sidewalls of the nitride by van der Waals forces, a model supported by the consistency of the strain across many devices.

The quality factor of each device can be extracted from the full width half-maximum of each Lorentzian resonance peak. A plot of the quality factor of fundamental modes as a function of diameter is shown in Figure 3b. There is a clear dependence of quality factor on resonator diameter, and fitting this data to $Q \sim D^{\beta}$ yields $\beta = 1.1 \pm 0.1$. The highest quality factor observed was 2400 ± 300 for a device with 22.5 μm diameter (Figure 3b, inset). We note that there was one 30 μm device measured in this data set, but it is not shown in these plots because it contained a significant rip. The quality factor of this ripped device was measured to be 1030 ± 150.

As a result of the dependence of both Q and frequency on diameter, Q must also be related to frequency, as shown in Figure 3c. To disentangle the effects of diameter and frequency on quality factor, we measure the quality factor of higher order modes of many membranes. Figure 4 shows the results of these measurements. With the possible exception of the smallest membranes, quality factor is not highly dependent on modal frequency. Certainly, the variation of dissipation with frequency between modes is less than linear for all but the smallest membrane. We therefore surmise that size, rather than frequency, is the essential factor determining the Q of the membrane.

To compare the dissipation in graphene to that in other mechanical resonators, we return to our discussion of RQ product. Liu et al.[6] introduced this figure of merit to account for the decrease in quality factor with decreasing volume to surface area, and it is a relevant measure of the performance of NEMS against the common problem of surface-related losses. Taking the thickness of graphene to be 0.335 nm,[19] the highest RQ product of a graphene resonator measured here is roughly 14 000 nm^{-1}. In contrast, single crystal silicon nanomechanical devices[6] achieve at most RQ in the range 200−3000 nm^{-1}. High stress silicon nitride resonators, which were recently discovered to have exceptionally high RQ products, have achieved RQ products of at most 100 000 nm^{-1} for a 0.5 mm × 0.5 mm × 50 nm square membrane.[9] Like graphene quality factors, however, silicon nitride quality factors also depend on the size of the resonator.

dx.doi.org/10.1021/nl1042227 |*Nano Lett.* XXXX, XXX, 000–000

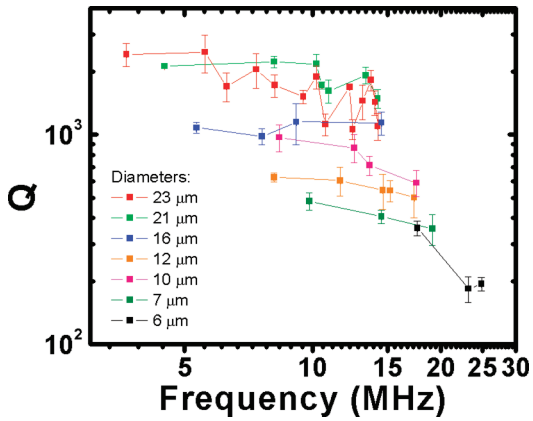

Figure 4. Quality factor as a function of modal frequency for resonators of different diameters. The dependence of dissipation on frequency is sublinear for all but the smallest resonator.

Thus, it is also relevant to compare our results to those of high stress nitride membranes of similar size, like the 15 μm diameter, 110 nm thick drumhead resonators reported in ref 29 (Q = 15 000; RQ = 270 nm^{-1}). That is, in drum resonators of comparable diameters, graphene has a quality factor to thickness ratio higher than that of high stress silicon nitride.

The origin of the dissipation in graphene resonators is currently unknown; however, the observations in this Letter provide some insight. We first discuss why we see high Q from the devices in this work and not for previously fabricated monolayer graphene doubly clamped beams, which have been studied as a function of length up to 6 μm with no reported dependence on size.[17] Although the fabrication methods used here are less invasive than those used to fabricate doubly clamped beams from CVD graphene (the graphene here is exposed only to PMMA, copper etchant, and water), we do not believe that better treatment is responsible for the improved quality factor, since monolayer graphene resonators made by exfoliation, the cleanest possible method, also had low Q (~80) at room temperature.[13] More likely, the improvement in quality factor is due to fixing the membranes on all sides, which, according to simulations, improves Q by eliminating "spurious edge modes."[30] The reproducible spectra of our membranes compared to those of doubly clamped membranes[17] lends further credence to this theory.

Even if fixing all sides of the membrane eliminates dissipation due to edge modes, we are confronting another source of dissipation that is dependent on size and not strongly dependent on modal frequency. We consider several candidate sources[31] of this dissipation in light of these observations. We find that the contribution from thermoelastic damping, which we calculate by treating the graphene as a clamped circular plate,[32] is too small to be important for our resonators. The dependence of the dissipation on size, or, equivalently, perimeter to area ratio, suggests that anchor losses may play a role in graphene. However, a recent model[29] of losses from phonon tunneling into the substrate gives dissipation estimates that are orders of magnitude too low, and it predicts a complicated behavior of quality factor as a function of mode that we do not observe here. A more probable candidate is surface-related effects, which seem likely to play a role for these ultrathin resonators given the increase in dissipation of most NEMS with increased surface to volume ratio. We note that both the size dependence and the modal frequency dependence of circular graphene membranes are qualitatively similar to the dissipation in doubly clamped silicon nitride beams,[7] which was found to be related to local strain in the resonators and possibly to coupling of the strain with surface defects.[33] Further modeling is required to examine these dissipation mechanisms. Measurements of the dissipation as a function of temperature should also prove revealing.

The high RQ products observed here demonstrate that large graphene resonators have the potential to be very sensitive to mass per unit area. A commercial quartz crystal microbalance can resolve approximately 400 pg cm^{-2},[34] while based on eq 1 and a study of the dynamic range achieved with our readout technique (see Supporting Information), a graphene resonator 12 μm in diameter could resolve 3 pg cm^{-2} (4 ag total mass). Further progress in biological functionalization[35] should enable specific detection with this sensitivity, which would be useful for biomedical sensing. Also, the limit of force sensitivity for these resonators is $dF = (4k_{\mathrm{eff}}\, k_{\mathrm{B}}T/\omega Q)^{1/2}$, where k_{eff} is the effective spring constant, k_{B} is the Boltzmann constant, T is temperature, and ω is frequency.[36] For our highest quality factor resonator, this limit is $dF \sim 200$ aN/Hz$^{1/2}$, which is high for room temperature operation. Additionally, because $k_{\mathrm{eff}} \sim m_{\mathrm{eff}}\omega^2$ is independent of diameter, and because we find empirically that ωQ is independent of diameter, this limit of force sensitivity is independent of the resonator area. Therefore, large-area graphene membrane resonators should enable very sensitive measurements of force per unit area.

This study provides information about dissipation in monolayer graphene resonators that was not accessible before the recent advances in graphene fabrication. We show that quality factor in tensile graphene drums is proportional to the diameter of the membrane. For our largest resonators, we observe RQ products as high as 14 000 nm^{-1}, which is better than that of even high stress silicon nitride resonators of comparable sizes. It therefore appears that relative to its low mass, graphene offers an excellent quality factor in addition to its high frequency and high electrical conductivity, making it an ideal material for NEMS.

■ ASSOCIATED CONTENT

Supporting Information. Raman spectrum and study of the dynamic range of a circular graphene resonator. This material is available free of charge via the Internet at http://pubs.acs.org.

■ AUTHOR INFORMATION

Corresponding Author

*Address: 205 Clark Hall, Cornell University, Ithaca, NY 14853. E-mail: hgc1@cornell.edu.

■ ACKNOWLEDGMENT

The authors thank Carlos Ruiz-Vargas, Jiwoong Park, Pinshane Huang, Vivek P. Adiga, and Tina M. Gonzalez for useful discussions. Fabrication was performed at the Cornell Nano-Scale Facility, a member of the National Nanotechnology Infrastructure Network, which is supported by the National Science Foundation (Grant ECS-0335765). This work was supported by the Cornell Center for Materials Research (CCMR) with funding from the Materials Research Science and Engineering Center Program of the National Science Foundation (cooperative agreement DMR 0520404), the MARCO Focused Research Center on Materials, Structures, and Devices, and the AFOSR MURI.

REFERENCES

(1) Ilic, B.; Craighead, H. G.; Krylov, S.; Senaratne, W.; Ober, C.; Neuzil, P. *J. Appl. Phys.* **2004**, *95* (7), 3694–3703.

(2) Mamin, H. J.; Rugar, D. *Appl. Phys. Lett.* **2001**, *79* (20), 3358–3360.

(3) LaHaye, M. D.; Buu, O.; Camarota, B.; Schwab, K. C. *Science* **2004**, *304* (5667), 74–77.

(4) Ekinci, K. L.; Huang, X. M. H.; Roukes, M. L. *Appl. Phys. Lett.* **2004**, *84* (22), 4469–4471.

(5) Ekinci, K. L.; Roukes, M. L. *Rev. Sci. Instrum.* **2005**, *76* (6), No. 061101.

(6) Liu, X.; Vignola, J. F.; Simpson, H. J.; Lemon, B. R.; Houston, B. H.; Photiadis, D. M. *J. Appl. Phys.* **2005**, *97* (2), No. 023524.

(7) Verbridge, S. S.; Parpia, J. M.; Reichenbach, R. B.; Bellan, L. M.; Craighead, H. G. *J. Appl. Phys.* **2006**, *99* (12), 8.

(8) Verbridge, S. S.; Craighead, H. G.; Parpia, J. M. *Appl. Phys. Lett.* **2008**, *92* (1), No. 013112.

(9) Wilson, D. J.; Regal, C. A.; Papp, S. B.; Kimble, H. J. *Phys. Rev. Lett.* **2009**, *103* (20), No. 207204.

(10) Rocheleau, T.; Ndukum, T.; Macklin, C.; Hertzberg, J. B.; Clerk, A. A.; Schwab, K. C. *Nature* **2010**, *463* (7277), 72–75.

(11) Sazonova, V.; Yaish, Y.; Ustunel, H.; Roundy, D.; Arias, T. A.; McEuen, P. L. *Nature* **2004**, *431* (7006), 284–287.

(12) Jensen, K.; Kim, K.; Zettl, A. *Nat. Nanotechnol.* **2008**, *3* (9), 533–537.

(13) Bunch, J. S.; van der Zande, A. M.; Verbridge, S. S.; Frank, I. W.; Tanenbaum, D. M.; Parpia, J. M.; Craighead, H. G.; McEuen, P. L. *Science* **2007**, *315* (5811), 490–493.

(14) Lee, C.; Wei, X. D.; Kysar, J. W.; Hone, J. *Science* **2008**, *321* (5887), 385–388.

(15) Chen, C. Y.; Rosenblatt, S.; Bolotin, K. I.; Kalb, W.; Kim, P.; Kymissis, I.; Stormer, H. L.; Heinz, T. F.; Hone, J. *Nat. Nanotechnol.* **2009**, *4* (12), 861–867.

(16) Singh, V.; Sengupta, S.; Solanki, H. S.; Dhall, R.; Allain, A.; Dhara, S.; Pant, P.; Deshmukh, M. M. *Nanotechnology* **2010**, *21* (16), No. 165204.

(17) van der Zande, A. M.; Barton, R. A; Alden, J. S.; Ruiz-Vargas, C. S.; Whitney, W. S.; Pham, P. H. Q.; Park, J.; Parpia, J. M.; Craighead, H. G.; McEuen, P. L. *Nano Lett.* **2010**, *10*, 4869–4873.

(18) Bunch, J. S.; Verbridge, S. S.; Alden, J. S.; van der Zande, A. M.; Parpia, J. M.; Craighead, H. G.; McEuen, P. L. *Nano Lett.* **2008**, *8* (8), 2458–2462.

(19) Aljishi, R.; Dresselhaus, G. *Phys. Rev. B* **1982**, *26* (8), 4514–4522.

(20) Robinson, J. T.; Zalalutdinov, M.; Baldwin, J. W.; Snow, E. S.; Wei, Z. Q.; Sheehan, P.; Houston, B. H. *Nano Lett.* **2008**, *8* (10), 3441–3445.

(21) Shivaraman, S.; Barton, R. A.; Yu, X.; Alden, J.; Herman, L.; Chandrashekhar, M. V. S.; Park, J.; McEuen, P. L.; Parpia, J. M.; Craighead, H. G.; Spencer, M. G. *Nano Lett.* **2009**, *9* (9), 3100–3105.

(22) Li, X. S.; Cai, W. W.; An, J. H.; Kim, S.; Nah, J.; Yang, D. X.; Piner, R.; Velamakanni, A.; Jung, I.; Tutuc, E.; Banerjee, S. K.; Colombo, L.; Ruoff, R. S. *Science* **2009**, *324* (5932), 1312–1314.

(23) Jiao, L. Y.; Fan, B.; Xian, X. J.; Wu, Z. Y.; Zhang, J.; Liu, Z. F. *J. Am. Chem. Soc.* **2008**, *130* (38), 12612–12613.

(24) Huang, P. Y.; Ruiz-Vargas, C. S.; Zande, A. M. v. d.; Whitney, W. S.; Garg, S.; Alden, J. S.; Hustedt, C. J.; Zhu, Y.; Park, J.; McEuen, P. L.; Muller, D. A. *Nature* **2011**, *469* (7330), 389−392.

(25) Carr, D. W.; Craighead, H. G. *J. Vac. Sci. Technol., B* **1997**, *15* (6), 2760–2763.

(26) Ilic, B.; Krylov, S.; Aubin, K.; Reichenbach, R.; Craighead, H. G. *Appl. Phys. Lett.* **2005**, *86* (19), 3.

(27) Weaver, W.; Timoshenko, S. P.; Young, D. H. *Vibrations Problems in Engineering*; Wiley: New York, 1990.

(28) Garcia-Sanchez, D.; van der Zande, A. M.; Paulo, A. S.; Lassagne, B.; McEuen, P. L.; Bachtold, A. *Nano Lett.* **2008**, *8* (5), 1399–1403.

(29) Wilson-Rae, I.; Barton, R. A.; Verbridge, S. S.; Southworth, D. R.; Ilic, B.; Craighead, H. G.; Parpia, J. M. *Phys. Rev. Lett.* **2011**, *106* (4), No. 047205.

(30) Kim, S. Y.; Park, H. S. *Nano Lett.* **2009**, *9* (3), 969–974.

(31) Seoanez, C.; Guinea, F.; Castro, A. H. *Phys. Rev. B* **2007**, *76* (12), No. 125427.

(32) Sun, Y. X.; Saka, M. *J. Sound Vib.* **2010**, *329* (3), 328–337.

(33) Unterreithmeier, Q. P.; Faust, T.; Kotthaus, J. P. *Phys. Rev. Lett.* **2010**, *105* (2), No. 027205.

(34) Zourob, M.; Elwary, S.; Turner, A. *Principles of Bacterial Detection: Biosensors, Recognition Receptors, and Microsystems*; Springer: New York, 2008.

(35) Cui, Y.; Kim, S. N.; Jones, S. E.; Wissler, L. L.; Naik, R. R.; McAlpine, M. C. *Nano Lett.* **2010**, *10* (11), 4559–4565.

(36) Yasumura, K. Y.; Stowe, T. D.; Chow, E. M.; Pfafman, T.; Kenny, T. W.; Stipe, B. C.; Rugar, D. *J. Microelectromech. Syst.* **2000**, *9* (1), 117–125.